ISSN 1063-7761, Journal of Experimental and Theoretical Physics, 2014, Vol. 119, No. 1, pp. 124–137. © Pleiades Publishing, Inc., 2014.
Original Russian Text © V.V. Val'kov, S.V. Aksenov, E.A. Ulanov, 2014, published in Zhurnal Eksperimental'noi i Teoreticheskoi Fiziki, 2014, Vol. 146, No. 1, pp. 144–159.

ELECTRONIC PROPERTIES OF SOLID

Inelastic Tunnel Transport of Electrons through an Anisotropic Magnetic Structure in an External Magnetic Field

V. V. Val'kov[a,*], S. V. Aksenov[a,], and E. A. Ulanov[b]**

[a] *Kirensky Institute of Physics, Siberian Branch, Russian Academy of Sciences, Krasnoyarsk, 660036 Russia*
[b] *Siberian Aerospace University, Krasnoyarsk, 660014 Russia*
**e-mail: vvv@iph.krasn.ru*
***e-mail: asv86@iph.krasn.ru*

Received December 19, 2013

Abstract—Quantum transport of electrons through a magnetic impurity located in an external magnetic field and affected by a substrate is considered using the Keldysh diagram technique for the Fermi and Hubbard operators. It is shown that in a strongly nonequilibrium state induced by multiple reflections of electrons from the impurity, the current–voltage (I–V) characteristic of the system contains segments with a negative conductivity. This effect can be controlled by varying the anisotropy parameter of the impurity center as well as the parameters of coupling between the magnetic impurity and metal contacts. The application of the magnetic field is accompanied by an increase in the number of Coulomb steps in the I–V curve of the impurity. The effect of appreciable magnetoresistance appears in this case. We demonstrate the possibility of switching between magnetic impurity states with different total spin projection values in the regime of asymmetric coupling of this impurity with the contacts.

DOI: 10.1134/S1063776114060065

1. INTRODUCTION

Because the application of semiconducting field transistors has almost reached its technological limit, it has become necessary to for alternative materials that for new-generation electronic devices. Such promising systems include nanoheterostructures containing layers of a ferromagnetic metal [1] or magnetic semiconductors [2], as well as Josephson-type systems [3–5]. In data recording and storage, this problem can be solved, in particular, by designing new memory systems that would have better basic parameters (such as the size, energy consumption, reading time, and number of rewriting cycles) as compared to those of existing semiconducting samples (e.g., flash memory cards).

As a result of considerable advances in technology and substantial enhancement of experimental potential, magnetic atomic and molecular complexes, as well as individual particles, have become objects of keen interest in recent decades. Such structures are either adsorbed in the region of a break junction [6] or are located on the surface; they are probed by a scanning tunnel microscope (STM) [7]. Sometimes, a magnetic ion is placed into a quantum dot (QD) [8]. The role of such a center can be played by an atom of a transition or rare-earth metal (e.g., Co, Mn, Fe, or Ce), as well as a molecule in which the magnetic core is surrounded by ligands (e.g., phthalocyanines of Co and Fe; Mn_{12}).

STM experiments with magnetic systems on the atomic scale have revealed a number of resonance effects in the transport characteristics of these structures. The origin of such peculiarities is associated with inelastic scattering of electrons due to the interaction of their spins with the spin moments of the atomic structure [9]. It was shown that the spin-flip scattering of transported electrons from the potential profile of the structure makes it possible to control its magnetic states [10]. The experiments demonstrated that the spin state of systems in principle can be controlled down to an individual atom. In particular, the possibility of recording and reading information on an antiferromagnetic chain of eight atoms by passing a spin-polarized current from the STM point contacting an individual atom of such a chain was demonstrated in [11]. Thus, a magnetic bit on the atomic scale has been realized without applying an external magnetic field for recording information, which is required for magnetic domains in contemporary hard disks.

Experimental data show that in the theoretical analysis of transport properties of an atomic-scale system, the processes of the transition of these systems into excited states should be taken into account. Such transitions are induced due to the interaction of electrons being transported with the charge and spin degrees of freedom of the system. As a result, a situation arises in which the passage of the tunnel current leads to a distribution of the energy level populations of the system, which differs significantly from the

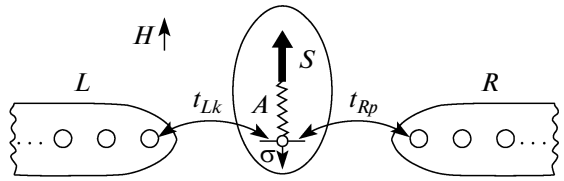

Fig. 1. Magnetic impurity with spin S located between two metal contacts.

equilibrium distribution. In particular, the inclusion of charge and spin correlations under nonequilibrium conditions leads to such effects as the Coulomb blockade and Kondo resonance [12, 13]. It was shown earlier that the existence of vibrational degrees of freedom of a molecule is manifested as a modification of its current–voltage (I–V) characteristics due to excitation of a molecule by the tunnel current passing through it [14, 15].

Since atomic-scale structures in actual conditions are in a tunnel junction with metal electrodes, the statistical properties of electron ensembles in such electron ensembles should be taken into account. This means that electron scattering from a magnetic structure should be calculated taking into account the fact that the interaction of previous electrons with the structure could generally change its potential profile. As a result of multiple repetition of scattering of electrons from the renormalized potential profile of the structure, a nonequilibrium distribution of occupancy of the states that sets in a magnetic structure differs significantly from the initial equilibrium distribution. Accordingly, some I–V characteristics are renormalized and become dependent on the properties of the tunnel-current-induced nonequilibrium state of the magnetic structure, indicating the existence of transitions between excited states [10]. An additional factor that should be taken into account in describing the transport properties of magnetic atomic structures is the influence of the crystal surroundings in the magnetic properties of the adsorbate. In particular, depending on the strength and type of the bond between an adatom and the substrate, the anisotropy type may change [16] or the magnetic moment can be screened due to Kondo correlations [17].

In this study, we solve the problem of the I–V characteristic of an adsorbed atom that exhibits anisotropy in magnetic properties due to the effect of the substrate in an external magnetic field H at a finite temperature with allowance for the above-mentioned factors. The results of calculating the I–V characteristic for $H = 0$ were briefly described in [18]. The nonuniform spacing of a large number of states of the "magnetic atom + electrons" system is taken into account exactly using the atomic representation and the description of dynamic processes in terms of the Hubbard operators [12, 19, 20]. The nonequilibrium occupation numbers for the states of the magnetic structure under investigation is calculated using the solution to a closed system of kinetic equations obtained using the Keldysh diagram technique [21] both for the Fermi and Hubbard operators [19, 20]. It is modified by introducing the Keldysh contour for the nonequilibrium case [22, 23]. Such an approach makes it possible to take into account multiple scattering of electrons in all orders of perturbation theory in the parameter of coupling of the structure to contacts, and to obtain the expression for current satisfying the necessary symmetry properties [15]. Calculations show that the I–V characteristic of a magnetic impurity in the tunnel regime has segments with a negative differential conductivity (NDC). It is noted that a change in the anisotropy parameter of the impurity and the asymmetry of the coupling with the contacts can enhance the NDC effect. It is shown that the application of magnetic field increases the number of Coulomb steps and contributed to the occurrence of considerable magnetoresistance of the system.

2. HAMILTONIAN OF THE SYSTEM

Let us consider tunnel transport of electrons through a magnetic impurity with spin $S = 1$ in an external magnetic field $\mathbf{H}$ in the geometry shown in Fig. 1. Such a configuration corresponds to some of the above-mentioned experiments, in which transported electrons interact with magnetic impurities.

The Hamiltonian of such a system in external magnetic field H can be written in the form

$$\hat{H} = \hat{H}_0 + \hat{T} + \hat{V}_\varphi, \quad \hat{H}_0 = \hat{H}_L + \hat{H}_D + \hat{H}_R. \qquad (1)$$

Operators $\hat{H}_L$ and $\hat{H}_R$ appearing in the expression for $\hat{H}_0$ describe conduction electrons in the left and right metal contacts, respectively,

$$\hat{H}_L = \sum_{k\sigma} \xi_{Lk\sigma} c^\dagger_{k\sigma} c_{k\sigma}, \quad \hat{H}_R = \sum_{p\sigma} \xi_{Rp\sigma} d^\dagger_{p\sigma} d_{p\sigma}, \qquad (2)$$

where $c_{k\sigma}(d_{p\sigma})$ is the electron annihilation operator for the left (right) contact with wavevector $k(p)$ and spin projection σ; $\xi_{Lk\sigma} = \varepsilon_{Lk} - \sigma g_e \mu_B H - \mu$ and $\xi_{Rp\sigma} = \varepsilon_{Rp} - \sigma g_e \mu_B H - \mu$ are the one-electron energies in the left and right contacts, respectively, which are measured from chemical potential μ and take into account energy splitting in the electron spin projection $\sigma = \pm 1/2$ in the magnetic field; g_e is the electron g factor in the contacts, and μ_B is the Bohr magneton. From here on, we will assume that the contacts are one-band paramagnetic metals with bandwidth $W = 4|t| \sim 1$ eV (t is the overlap integral for the electron wavefunctions at the neighboring sites in the contacts) considerably exceeding the characteristic energy parameters in the system.

The second term in the expression for $\hat{H}_0$ is the Hamiltonian of the magnetic impurity (structure),

$$\hat{H}_D = \sum_\sigma \xi_{d\sigma} n_\sigma + U n_\uparrow n_\downarrow + D(S^z)^2 - S^z g\mu_B H + A(\boldsymbol{\sigma}\cdot\mathbf{S}), \quad (3)$$

where $\xi_{d\sigma} = \varepsilon_d - \sigma g_e \mu_B H - \mu$ is the spin-dependent energy (measured from the chemical potential) of an electron located on the impurity in external magnetic field $\mathbf{H}$; ε_d is the initial one-electron energy of the impurity atom; $n_\sigma = a_\sigma^\dagger a_\sigma$ is the operator of the number of electrons at an impurity center with spin projection σ; $a_\sigma^\dagger (a_\sigma)$ is the electron creation (annihilation) operator on the impurity atom with spin projection σ; and parameter U characterizes the Hubbard repulsion of two electrons with opposite spin projections. The effect of the crystal surroundings on the magnetic properties of the impurity [17] is simulated by introducing the uniaxial anisotropy parameter D. The action of the magnetic field on the energy structure of an impurity center with the effective g factor is described by the last but one term in Eq. (3). The interrelation between the spin degrees of freedom of the electron being transported and the impurity atom is effected via the mechanism of $s - d(f)$ exchange coupling. It is described by the last term in Eq. (3), in which $\mathbf{S}$ is the vector operator of the spin moment of the impurity and $\boldsymbol{\sigma}$ is the vector spin operator of the transported electron. The intensity of $s - d(f)$ exchange coupling is determined by parameter A. It is well known that scalar product $\boldsymbol{\sigma}\cdot\mathbf{S}$ contains the operator terms corresponding to inclusion of spin-flip processes, in which the spin projections of the impurity and the electron change simultaneously; the total value of the z projection of the spin of the entire system is conserved. The importance of such processes is, in particular, due to the fact that the potential profile of the scattering center changes owing to these processes. This is manifested, for example, in the induction of the Fano effect [24]. It will be shown below that such processes in our case considerably affect the I–V characteristic of the system.

The coupling of the magnetic impurity with the metal contacts is described by the second term of the Hamiltonian of system (1) by taking into account electron tunneling between the contacts and the magnetic impurity:

$$\hat{T} = \sum_{k\sigma} t_{Lk} c_{k\sigma}^\dagger a_\sigma + \sum_{p\sigma} t_{Rp} d_{p\sigma}^\dagger a_\sigma + \text{h.c.} \quad (4)$$

Here, t_{Lk} and t_{Rp} are the parameters of coupling of the left and right contacts with the impurity, respectively.

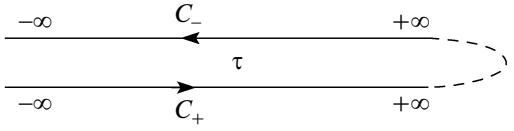

Fig. 2. Temporal Keldysh contour C.

Last term $\hat{V}_\varphi$ in the total Hamiltonian of the system, which is due to the application to the metal contacts of bias voltage V, is defined as

$$\hat{V}_\varphi = \sum_\sigma (eV/2) a_\sigma^\dagger a_\sigma + \sum_{p\sigma} (eV) d_{p\sigma}^\dagger d_{p\sigma}. \quad (5)$$

3. HILBERT SPACE OF STATES OF AN ISOLATED SYSTEM AND ATOMIC REPRESENTATION

Calculation of the transport characteristics of the system using the Keldysh method [21] is based on application of the diagram form of perturbation theory for a nonequilibrium system, in which the time integrals appearing in the S matrix are defined on Keldysh contour C (Fig. 2). The structure of the diagram series is known to depend not only on the perturbation operator in the interaction representation, but also on the zeroth-approximation Hamiltonian. If we describe the Hamiltonian of the system in the initial language of Fermi second-quantization operators, as well as spin operators, the above formulas lead to the conclusion that the Hamiltonian of the system is not a diagonal operator. This considerably complicates averaging over the density matrix corresponding to the unperturbed Hamiltonian in the above representation.

This technical difficulty can be overcome by passing to the atomic representation, in which $\hat{H}_D$ becomes a diagonal operator. It is well known that the construction of such a representation involves the complete orthonormal set of wavefunctions $|\psi_n\rangle$ (in our case, $n = 1, 2, ..., 12$) as the basis vectors of the Hilbert space of states of the system. In this case, functions $|\psi_n\rangle$ satisfy the Schrödinger equation $\hat{H}_D|\psi_n\rangle = E_n|\psi_n\rangle$ with operator $\hat{H}_D$, in which bias voltage V is zero. If we introduce Hubbard operators $X^{nm} = |\psi_n\rangle\langle\psi_n|$, the Hamiltonian of the system in the atomic representation constructed in this wave assumes the diagonal form

$$\hat{H}_D = \sum_{n=1}^{12} E_n X^{nn}. \quad (6)$$

Since the operator of the number of electrons in the system commutes with $\hat{H}_D$, the basis vectors of the space of states of the system can be like sets of vectors

in each of which the basis vector describes a state with a fixed number of electrons in the system (0, 1, or 2). Accordingly, the Hilbert space of the states of the system splits into three sectors.

The sector with zero number of electrons is defined as the space of states specified by an arbitrary linear superposition of three basis vectors ($S = 1$):

$$\psi_1 = |0, 0\rangle, \quad \psi_{2,3} = |0, \pm 1\rangle. \tag{7}$$

The ket-vector on the right-hand side of these and subsequent expressions is used to identify the states with a preset number of electrons and the spin projection of the impurity. The first index of the ket-vector for this sector corresponds to the absence of electrons in the system. The second subscript on the ket-vector indicates the projection of the impurity spin.

The one-fermion sector of the Hilbert space is defined by a set of six eigenfunctions of operator $\hat{H}_D$:

$$\begin{aligned}
\psi_4 &= \cos\Theta_+|\uparrow, 0\rangle - \sin\Theta_+|\downarrow, +1\rangle,\\
\psi_5 &= \cos\Theta_-|\downarrow, 0\rangle - \sin\Theta_-|\uparrow, -1\rangle,\\
\psi_6 &= \mathrm{sgn}(A)(\sin\Theta_+|\uparrow, 0\rangle - \cos\Theta_+|\downarrow, +1\rangle),\\
\psi_7 &= \mathrm{sgn}(A)(\sin\Theta_-|\downarrow, 0\rangle + \cos\Theta_-|\uparrow, -1\rangle),\\
\psi_8 &= |\uparrow, +1\rangle, \quad \psi_9 = |\downarrow, -1\rangle,
\end{aligned} \tag{8}$$

where the first index on the ket-vector shows the spin orientation of the electron located on the impurity. The expansion coefficients have the form

$$\begin{aligned}
\sin\Theta_\pm &= \mathrm{sgn}(A)\sqrt{\frac{1+x_\pm}{2}},\\
\cos\Theta_\pm &= \sqrt{\frac{1-x_\pm}{2}},\\
x_\pm &= \Delta_\pm/\nu_\pm, \quad \nu_\pm = \sqrt{\Delta_\pm^2 + A^2/2},\\
\Delta_\pm &= \Delta \pm (g/2-1)h, \quad \Delta = A/4 - D/2,\\
h &= \mu_B H.
\end{aligned} \tag{9}$$

The effect of the magnetic field is manifested in the dependence of these expressions on h. For real systems, the conditions in which the energy of the Zeeman interaction is lower than the parameters of the model hold in most cases. Then in the approximation linear in h, we can easily establish the explicit dependence of the expansion coefficients on the magnetic field:

$$\begin{aligned}
\sin\Theta_\pm &\approx \sin\Theta \pm \left(\frac{g}{2}-1\right)h\frac{1-x}{2\nu}\sin\Theta,\\
\cos\Theta_\pm &\approx \cos\Theta \mp \left(\frac{g}{2}-1\right)h\frac{1+x}{2\nu}\cos\Theta,\\
\sin\Theta &= \mathrm{sgn}(A)\sqrt{\frac{1+x}{2}}, \quad \cos\Theta = \sqrt{\frac{1-x}{2}},
\end{aligned} \tag{10}$$

$$x = \frac{\Delta}{\nu}, \quad \nu = \sqrt{\Delta^2 + \frac{A^2}{2}}.$$

The basis vectors of the two-electron sector are defined as

$$\psi_{10} = |2, 0\rangle, \quad \psi_{11,12} = |2, \pm 1\rangle. \tag{11}$$

The energy eigenvalues E_i of the system ($i = 1, 2, \ldots, 12$) corresponding to eigenstates ψ_i can be written in the form

$$\begin{aligned}
E_1 &= 0, \quad E_{2(3)} = D \mp gh,\\
E_{4(5)} &= \xi_{d\uparrow(\downarrow)} - \Delta_\pm - \nu_\pm,\\
E_{6(7)} &= \xi_{d\uparrow(\downarrow)} - \Delta_\pm + \nu_\pm,\\
E_{8(9)} &= \xi_{d\uparrow(\downarrow)} + D + A/2 \mp gh,\\
E_{10} &= 2\xi_d + U, \quad E_{11(12)} = 2\xi_d + U + D \mp gh.
\end{aligned} \tag{12}$$

For one-fermion excitations of the magnetic impurity, transitions between states ψ_i for which the numbers of electrons differ by unity take place. For each spin projection, ten such transitions exist. In the given problem, the magnetic-field dependences of the energy differences of the above transitions play an important role. This is due to the fact that the energy splitting in one-fermion transitions in a magnetic field for electrons with different spin projections underlies the variation of the dependence of the occupation numbers on the electric field (see below) and determines the formation of additional steps on the I–V curve. Bearing this in mind, we can write the explicit dependence of transition energies on h with the above-mentioned accuracy. For $\sigma = +1/2$, we have

$$\begin{aligned}
E_{1,4} &= E_1 - E_4 \approx \Delta + \nu - \xi_d + g_+h,\\
E_{1,6} &\approx \Delta - \nu - \xi_d + g_-h,\\
E_{3,5} &\approx \Delta + \nu + D - \xi_d + g_-h,\\
E_{3,7} &\approx \Delta - \nu + D - \xi_d + g_+h,\\
E_{2,8} &= -(A/2 + \xi_d - h),\\
E_{4,11} &\approx -(\Delta + \nu + U + D + \xi_d) + g_-h,\\
E_{5,10} &\approx -(\Delta + \nu + U + \xi_d) + g_+h,\\
E_{6,11} &\approx -(\Delta - \nu + U + D + \xi_d) + g_+h,\\
E_{7,10} &\approx -(\Delta - \nu + U + \xi_d) + g_-h,\\
E_{9,12} &= -(U - A/2 + \xi_d - h),
\end{aligned} \tag{13}$$

where $g_\pm = g/2 \pm \Delta(g/2-1)/\nu$. For $\sigma = -1/2$, we have

$$\begin{aligned}
E_{1,5} &\approx \Delta + \nu - \xi_d - g_+h,\\
E_{1,7} &\approx \Delta - \nu - \xi_d - g_-h,\\
E_{2,4} &\approx \Delta + \nu + D - \xi_d - g_-h,\\
E_{2,6} &\approx \Delta - \nu + D - \xi_d - g_+h,\\
E_{3,9} &= -(A/2 + \xi_d + h),\\
E_{4,10} &\approx -(\Delta + \nu + U + \xi_d) - g_+h,\\
E_{5,12} &\approx -(\Delta + \nu + U + D + \xi_d) - g_-h,
\end{aligned} \tag{14}$$

$$E_{6,10} \approx -(\Delta - \nu + U + \xi_d) - g_- h,$$
$$E_{7,12} \approx -(\Delta - \nu + U + D + \xi_d) - g_+ h,$$
$$E_{8,11} = -(U - A/2 + \xi_d + h).$$

Using these formulas, we can easily write the atomic representation of Fermi operator a_σ in terms of the Hubbard operators introduced above:

$$a_\sigma = \sum_{n,m} \langle \psi_n | a_\sigma | \psi_m \rangle X^{n,m} \equiv \sum_{n,m} \gamma_\sigma(n,m) X^{n,m} \equiv \sum_\alpha \gamma_\sigma(\alpha) X^\alpha. \quad (15)$$

To simplify the form of subsequent expressions, we have introduced the representation parameters $\gamma_\sigma(n, m) = \langle \psi_n | a_\sigma | \psi_m \rangle$ and have passed from the summation over two indices (n, m) to single index $\alpha(n, m)$ [20]. Taking into account the real nature of $\gamma_\sigma(n, m)$ (see below), we find that the following representation is realized for the creation operator:

$$a_\sigma^\dagger = \sum_\alpha \gamma_\sigma(\alpha) X^{-\alpha}, \quad -\alpha(n,m) = \alpha(m,n). \quad (16)$$

Evaluating matrix elements $\langle \psi_n | a_\sigma | \psi_m \rangle$, we obtain

$$\begin{aligned} a_\uparrow &= [\mathrm{sgn}(A) X^{1,6} - X^{4,11}] \sin\Theta_+ \\ &+ [X^{1,4} + \mathrm{sgn}(A) X^{6,11}] \cos\Theta_+ + X^{2,8} \\ &+ [\mathrm{sgn}(A) X^{7,10} - X^{3,5}] \sin\Theta_- \\ &+ [X^{5,10} + \mathrm{sgn}(A) X^{3,7}] \cos\Theta_- + X^{9,12}, \\ a_\downarrow &= -[X^{2,4} + \mathrm{sgn}(A) X^{6,10}] \sin\Theta_+ \\ &+ [\mathrm{sgn}(A) X^{2,6} - X^{4,10}] \cos\Theta_+ + X^{3,9} \\ &+ [\mathrm{sgn}(A) X^{1,7} + X^{5,12}] \sin\Theta_- \\ &+ [X^{1,5} - \mathrm{sgn}(A) X^{7,12}] \cos\Theta_- - X^{8,11}. \end{aligned} \quad (17)$$

Comparing expressions (17) and (15), we can determine the values of nonzero parameters $\gamma_\uparrow(\alpha)$ and $\gamma_\downarrow(\alpha)$ of the representation.

4. FORMULA FOR CURRENT AND SPECTRAL FUNCTIONS OF THE SYSTEM

We will calculate tunnel current I through a magnetic impurity using the nonequilibrium Keldysh diagram technique [21], in which the role of the unperturbed operator is played by operator H_0 alone, and all perturbations are transferred to the tunneling operator. This is performed using the unitary transformation [22], as a result of which we pass from density matrix $\rho(t)$ to density matrix $\rho_\varphi(t)$:

$$\rho_\varphi(t) = \exp(-iV_\varphi t)\rho(t)\exp(iV_\varphi t). \quad (18)$$

Here and below, $\hbar = 1$. Then the tunneling operator acquires the time dependence

$$\hat{T}_\varphi(t) = \sum_{k\sigma} t_{Lk} e^{-ieVt/2} c_{k\sigma}^\dagger a_\sigma + \sum_{p\sigma} t_{Rp} e^{+ieVt/2} d_{p\sigma}^\dagger a_\sigma + \mathrm{h.c.} \quad (19)$$

Consequently, the expression for calculating current I also contains the temporal factor,

$$I = e\left\langle \frac{d\hat{N}_L}{dt} \right\rangle = ie\sum_{k\sigma} t_{Lk} (\langle a_\sigma^\dagger c_{k\sigma} \rangle e^{ieVt/2} - \mathrm{h.c.}), \quad (20)$$

where $\hat{N}_L = \sum_{k\sigma} c_{k\sigma}^\dagger c_{k\sigma}$ is the operator of the number of electrons in the left contact. Angle brackets denote averaging with density matrix $\rho_\varphi(t)$.

Following [21], we introduce the scattering matrix

$$S_C = T_C \exp\left\{ -i \int_C \hat{T}_I(\tau) d\tau \right\}, \quad (21)$$

where the tunneling operator is written in the interaction representation:

$$\hat{T}_I(\tau) = \sum_{k\sigma,\alpha} t_{Lk} \gamma_\sigma(\alpha) [e^{-ieV\tau/2} c_{k\sigma}^\dagger(\tau) X^\alpha(\tau) + \mathrm{h.c.}] + \sum_{p\sigma,\alpha} t_{Rp} \gamma_\sigma(\alpha) [e^{ieV\tau/2} d_{p\sigma}^\dagger(\tau) X^\alpha(\tau) + \mathrm{h.c.}]. \quad (22)$$

The integration in formula (21) is carried out over the Keldysh contour shown in Fig. 2. The operator of ordering in T_C is also defined on this contour [21]. In writing tunneling operator $\hat{T}_I(t)$, we used the transition from operators a_σ to the Hubbard operators. This is due to the fact that the time dependence $X^\alpha(\tau)$, as well as of operators $c_{k\sigma}(\tau)$ and $d_{p\sigma}(\tau)$ in the interaction representation, can be reduced to multiplication by the c-numerical function, while this rule does not exist for $a_\sigma(\tau)$ (this prevents from the construction of the Feynman diagram technique using operators a_σ). If $\alpha = \alpha(n, m)$, we have $X^\alpha(\tau) = X^\alpha \exp[i(E_n - E_m)\tau] \equiv X^\alpha \exp[iE_\alpha \tau]$. Such a simple time dependence makes it possible to formulate the Wick theorem required for obtaining recurrent relations in expanding the mean value of the product of the Hubbard operators from the zeroth-order density matrix.

Let us define four families of nonequilibrium Green's functions:

$$\begin{aligned} R^{ab}_{k\sigma,\alpha}(\tau,\tau') &= -i\langle T_C c_{k\sigma}(\tau_a)X^{-\alpha}(\tau'_b)S_C\rangle_0,\\ R^{ab}_{\alpha,k\sigma}(\tau,\tau') &= -i\langle T_C X^{\alpha}(\tau_a)c^{\dagger}_{k\sigma}(\tau'_b)S_C\rangle_0,\\ D^{ab}_{\alpha,\beta}(\tau,\tau') &= -i\langle T_C X^{\alpha}(\tau_a)X^{-\beta}(\tau'_b)S_C\rangle_0,\\ G^{ab}_{Lk\sigma}(\tau,\tau') &= -i\langle T_C c_{k\sigma}(\tau_a)c^{\dagger}_{k\sigma}(\tau'_b)\rangle_0, \end{aligned} \tag{23}$$

for which each superscript a and b can assume two values "+" or "–." The first superscript a corresponds to time τ_a of the first operator appearing in the mean value ordered over the Keldysh contour. This means that for $a = +(-)$, operator $c_{k\sigma}(\tau_a)$ or $X^{\alpha}(\tau_a)$ in the interaction representation is taken at instant τ on the upper (lower) branch of the Keldysh contour. Analogously, for $b = +(-)$, operator $X^{-\alpha}(\tau'_b)$ or $c^{\dagger}_{k\sigma}(\tau'_b)$ is taken at instant τ' on the lower (upper) branch of the Keldysh contour.

Using representations (15) and (16) and functions $R^{ab}_{k\sigma,\alpha}$ and $R^{ab}_{\alpha,k\sigma}$ introduced above, we find that the expression for the current can be written in the form

$$\begin{aligned} I = e\sum_{k\sigma,\alpha} t_{Lk}\gamma_{\sigma}(\alpha)\{e^{ieVt/2}R^{++}_{Lk\sigma,\alpha}(t,t+\delta)\\ - e^{-ieVt/2}R^{++}_{\alpha,Lk\sigma}(t,t+\delta)\}, \quad \delta \longrightarrow +0. \end{aligned} \tag{24}$$

Expanding scattering matrix S_C in relations (23), we can easily verify the validity of the equations:

$$\begin{aligned} R^{++}_{k\sigma,\alpha}(t,t') = \sum_{\beta} t_{Lk}\gamma_{\sigma}(\beta)\\ \times \int_{-\infty}^{\infty} d\tau\{G^{++}_{Lk\sigma}(t-\tau)D^{++}_{\alpha\beta}(\tau-t')\\ - G^{+-}_{Lk\sigma}(t-\tau)D^{-+}_{\alpha\beta}(\tau-t')\}e^{-ieV\tau/2},\\ R^{++}_{\alpha,k\sigma}(t,t') = \sum_{\beta} t_{Lk}\gamma_{\sigma}(\beta)\\ \times \int_{-\infty}^{\infty} d\tau\{D^{++}_{\alpha\beta}(t-\tau)G^{++}_{Lk\sigma}(\tau-t')\\ - D^{+-}_{\alpha\beta}(t-\tau)G^{-+}_{Lk\sigma}(\tau-t')\}e^{ieV\tau/2}. \end{aligned} \tag{25}$$

Using these equations and performing the Fourier transformation over temporal arguments, we can obtain the following convenient expression for the current:

$$\begin{aligned} I = e\sum_{\sigma}\int_{-\infty}^{\infty}\frac{d\omega}{2\pi}\Big[Q^{-+}_{\sigma}(\omega)W^{+-}_{\sigma}\Big(\omega-\frac{eV}{2}\Big)\\ - Q^{+-}_{\sigma}(\omega)W^{-+}_{\sigma}\Big(\omega-\frac{eV}{2}\Big)\Big]. \end{aligned} \tag{26}$$

Here, we have introduced the spectral functions of the system,

$$W^{ab}_{\sigma}(\omega) = \sum_{\alpha\beta}\gamma_{\sigma}(\alpha)\gamma_{\sigma}(\beta)D^{ab}_{\alpha\beta}(\omega), \tag{27}$$

as well as the spectral functions for the tunnel coupling of the left contact with the system:

$$Q^{ab}_{\sigma}(\omega) = \sum_{k} t^2_{Lk}G^{ab}_{Lk\sigma}(\omega), \tag{28}$$

where $G^{ab}_{Lk\sigma}$ are the initial Green functions of the left contact:

$$\begin{aligned} G^{++}_{Lk\sigma}(\omega) &= \frac{n_{Lk\sigma}}{\omega-\xi_{Lk\sigma}-i\delta}+\frac{1-n_{Lk\sigma}}{\omega-\xi_{Lk\sigma}+i\delta},\\ G^{+-}_{Lk\sigma}(\omega) &= 2\pi i n_{Lk\sigma}\delta(\omega-\xi_{Lk\sigma}),\\ G^{--}_{Lk\sigma}(\omega) &= -\frac{n_{Lk\sigma}}{\omega-\xi_{Lk\sigma}+i\delta}-\frac{1-n_{Lk\sigma}}{\omega-\xi_{Lk\sigma}-i\delta},\\ G^{-+}_{Lk\sigma}(\omega) &= 2\pi i(n_{Lk\sigma}-1)\delta(\omega-\xi_{Lk\sigma}). \end{aligned} \tag{29}$$

Here,

$$n_{Lk\sigma} = \left\{1+\exp\left[\frac{\varepsilon_{Lk\sigma}-\mu}{T}\right]\right\}^{-1}.$$

Expression (26) shows that to determine the tunnel current, we must solve the problem of calculating spectral functions $W^{+-}_{\sigma}(\omega)$ and $W^{-+}_{\sigma}(\omega)$ of the system. It should be noted that the sums over α and β appearing in the definitions correspond to the inclusion of the contributions to the current from the transitions of the system between its states.

5. CALCULATION OF SPECTRAL FUNCTIONS OF THE SYSTEM

The derivation of equations for Green's functions $D^{ab}_{\alpha\beta}$ can be simplified taking into account the following two factors. First, operator H_0 is additive relative to the subsystems of two contacts and the system. Therefore, the mean value of the product of the Fermi and Hubbard operators splits into the product of the mean values, each of which contains an operator of only one type. The second factor appears due to the fact that the terms of the series for $D^{ab}_{\alpha\beta}(\tau-\tau')$ appearing as a result

of expansion of density matrix S_C vanish when operator $\hat{T}_I$ on average appears an odd number of times. The mean values of the products of the Fermi operators in even-order terms can easily be evaluated. As a result, the infinite series can be contracted into an exponential so that the definition of $D^{ab}_{\alpha\beta}$ contains the renormalized scattering matrix $\tilde{S}_C$:

$$D^{ab}_{\alpha\beta}(\tau-\tau') = -i\langle T_C X^{\alpha}(\tau_a) X^{-\beta}(\tau'_b)\tilde{S}_C\rangle_0, \qquad (30)$$

which can be defined from the effective interaction corresponding to only the subsystem of the system and expressed in terms of the Hubbard operators:

$$\tilde{S}_C = T_C \exp\left\{-i\int_C d\tau_1 \int_C d\tau_2 \times \sum_{\alpha\beta}\tilde{V}_{\alpha\beta}(\tau_1-\tau_2)X^{-\alpha}(\tau_1)X^{\beta}(\tau_2)\right\}. \qquad (31)$$

It should be noted that an analogous procedure was used earlier to determine the Green's functions of quasi-localized electrons in the Anderson model [25].

The matrix elements of the effective interaction depend on two temporal arguments defined on the Keldysh contour:

$$\tilde{V}_{\alpha\beta}(\tau_1-\tau_2) = \sum_{\sigma}\gamma_{\sigma}(\alpha)\gamma_{\sigma}(\beta) \times \left\{\sum_k t^2_{Lk}\exp\left\{i\frac{eV}{2}(\tau_1-\tau_2)\right\}G_{Lk\sigma}(\tau_1-\tau_2) + \sum_p t^2_{Rp}\exp\left\{-i\frac{eV}{2}(\tau_1-\tau_2)\right\}G_{Rp\sigma}(\tau_1-\tau_2)\right\}. \qquad (32)$$

The above transformations show that in determining nonequilibrium Green's functions $D^{ab}_{\alpha\beta}$, we can use the diagram technique for the Hubbard operators [19, 20], modified in accordance with the Keldysh method [21].

It is important for further analysis that quantum transport of electrons involves scattering processes accompanied by a change in the state of the system. As a result, an electron arriving at the system from the left contact can pass to the right contact or return to the left contact, after which it can tunnel to the region to the system again. Such processes may initiate a transition of the system to excited states. Multiple scattering effects will be taken into account by retaining the terms of all orders in the parameters of tunnel coupling of the system with left and right contacts in perturbation theory series for $D^{ab}_{\alpha\beta}$. In diagrammatic language, this means that functions $D^{ab}_{\alpha\beta}$ must satisfy the system of equations in graph form well known for Hubbard

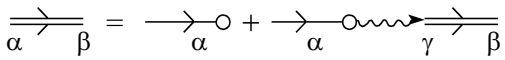

Fig. 3. System of equations for nonequilibrium functions $D_{\alpha\beta}$.

systems [19, 20], depicted in Fig. 3. Using the definition of Keldysh contour C (see Fig. 2), we find that the graph system of equations for $D^{ab}_{\alpha\beta}$ in the frequency representation (see Fig. 3) corresponds to the analytic system

$$D^{+-}_{\alpha\beta}(\omega) = \delta_{\alpha\beta}D^{+-}_{0\alpha}(\omega) + \sum_{\gamma}D^{++}_{0\alpha}(\omega) \times [\tilde{V}^{++}_{\alpha\gamma}(\omega)D^{+-}_{\gamma\beta}(\omega) - \tilde{V}^{+-}_{\alpha\gamma}(\omega)D^{--}_{\gamma\beta}(\omega)] + \sum_{\gamma}D^{+-}_{0\alpha}(\omega)[\tilde{V}^{--}_{\alpha\gamma}(\omega)D^{--}_{\gamma\beta}(\omega) - \tilde{V}^{-+}_{\alpha\gamma}(\omega)D^{+-}_{\gamma\beta}(\omega)],$$

$$D^{--}_{\alpha\beta}(\omega) = \delta_{\alpha\beta}D^{--}_{0\alpha}(\omega) + \sum_{\gamma}D^{-+}_{0\alpha}(\omega) \times [\tilde{V}^{++}_{\alpha\gamma}(\omega)D^{+-}_{\gamma\beta}(\omega) - \tilde{V}^{+-}_{\alpha\gamma}(\omega)D^{--}_{\gamma\beta}(\omega)] + \sum_{\gamma}D^{--}_{0\alpha}(\omega)[\tilde{V}^{--}_{\alpha\gamma}(\omega)D^{--}_{\gamma\beta}(\omega) - \tilde{V}^{-+}_{\alpha\gamma}(\omega)D^{+-}_{\gamma\beta}(\omega)]. \qquad (33)$$

The solution to this system of a large number of linear equations is substantially simplified if we take into account the following two factors. The first factor is that the dependence of the matrix elements of the interaction on the root vectors is of the split type:

$$\tilde{V}^{ab}_{\alpha\beta}(\omega) = \sum_{\sigma}\gamma_{\sigma}(\alpha)\gamma_{\sigma}(\beta)M^{ab}_{\sigma}(\omega), \qquad (34)$$

where

$$M^{ab}_{\sigma}(\omega) = Q^{ab}_{\sigma}\left(\omega+\frac{eV}{2}\right) + P^{ab}_{\sigma}\left(\omega-\frac{eV}{2}\right). \qquad (35)$$

In this case, using the technique described in [26], we can reduce the problem to solving a simple system of equations. The second factor is that we consider the collinear geometry of the problem, in which the external magnetic field is oriented along the anisotropy axis. In this case, the z projection of the total spin operator commutes with the Hamiltonian of the system, which allows us to classify the states of the system from the value of this projection. Then $\gamma_{\uparrow}(\alpha)\gamma_{\downarrow}(\alpha) \equiv 0$ for all transitions, and functions $L^{ab}_{\sigma\sigma'}(\omega) = \sum_{\alpha}\gamma_{\sigma}(\alpha)\gamma_{\sigma'}(\alpha)D^{ab}_{0\alpha}(\omega) = \delta_{\sigma\sigma'}L^{ab}_{\sigma}(\omega)$ are diagonal functions in the spin index. Therefore, the solution to the system of equations for the nonequilibrium Green's functions splits into two independent subsystems for each projection of the spin.

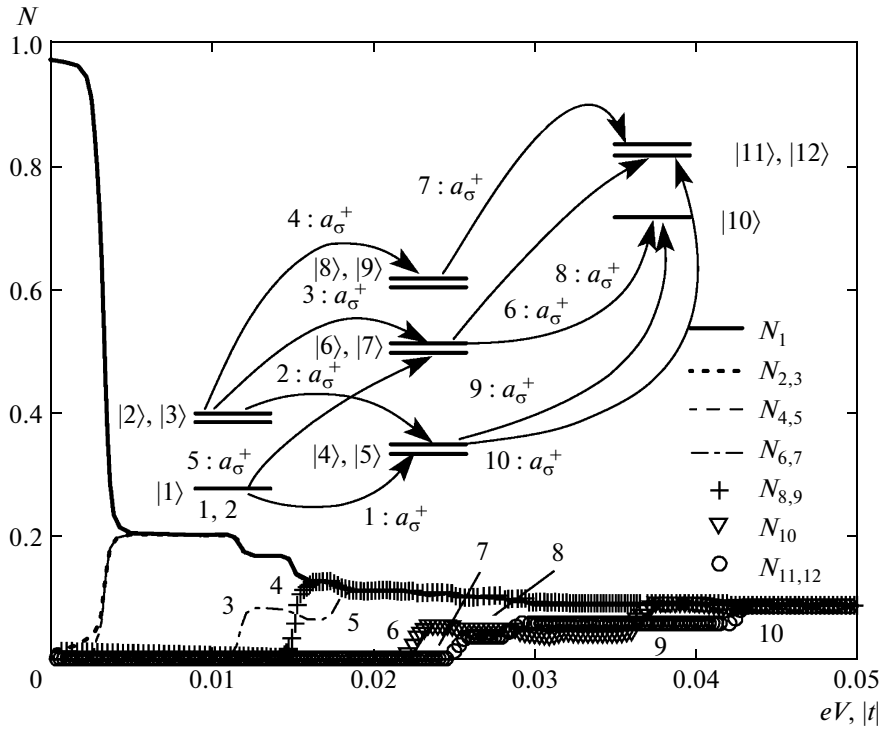

Fig. 4. Dependence of nonequilibrium occupation numbers on the electric field energy for parameters $t_L = t_R = t/100$, $\varepsilon_d = A = 0.005|t|$, $D = 0.003|t|$, $U = 0.01|t|$, $T = 1$ K, $g = 2$, and $h = 0$. The inset shows possible electron transitions between energy levels of the system.

In the noncollinear case, however, off-diagonal components $L^{ab}_{\uparrow\downarrow}(\omega)$ and $L^{ab}_{\uparrow\downarrow}(\omega) \neq 0$ differ from zero and the spectral functions of the system can be determined by solving the set of four equations.

Quantity $Q^{ab}_{\sigma}(\omega)$ was calculated earlier, and

$$P^{ab}_{\sigma}(\omega) = \sum_{p} t^2_{Rp} G^{ab}_{Rk\sigma}(\omega) \tag{36}$$

is the spectral function of the tunnel coupling of the right contact with the system.

Applying the Keldysh method [21] to system of equations (33) for the nonequilibrium Green's functions, we obtain

$$W^{+-}_{\sigma}(\omega) = -\frac{M^{+-}_{\sigma}(\omega)}{\Delta_{\sigma}(\omega)}, \tag{37}$$

where

$$\begin{aligned}\Delta_{\sigma}(\omega) = ([L^{++}_{\sigma}(\omega)]^{-1} - M^{++}_{\sigma}(\omega))\\ \times ([L^{--}_{\sigma}(\omega)]^{-1} - M^{--}_{\sigma}(\omega))\\ - M^{+-}_{\sigma}(\omega) M^{-+}_{\sigma}(\omega).\end{aligned} \tag{38}$$

The appearance of functions

$$L^{ab}_{\sigma}(\omega) = \sum_{\alpha} \gamma^2_{\sigma}(\alpha) D^{ab}_{0\alpha}(\omega)$$

in these expressions is associated with the possibility of transitions between eigenstates of the system. Initial functions $D^{ab}_{0\alpha}(\omega)$ of the system appearing in this expression are defined as

$$\begin{aligned}D^{++}_{0\alpha}(\omega) &= \frac{N_n}{\omega + E_{\alpha} + i\delta} + \frac{N_m}{\omega + E_{\alpha} - i\delta},\\ D^{+-}_{0\alpha}(\omega) &= 2\pi i N_m \delta(\omega + E_{\alpha}),\\ D^{--}_{0\alpha}(\omega) &= -\frac{N_n}{\omega + E_{\alpha} - i\delta} - \frac{N_m}{\omega + E_{\alpha} + i\delta},\\ D^{-+}_{0\alpha}(\omega) &= -2\pi i N_n \delta(\omega + E_{\alpha}).\end{aligned} \tag{39}$$

It should be noted that quantity E_{α} denotes the energy difference between levels n and m (i.e., $E_{\alpha} = E_n - E_m$ for $\alpha = \alpha(n, m)$). The effect of the magnetic field on the transition energies essential for the given problem is determined by formulas (13) and (14). A transition of the system from state n to state m becomes effective only when the value of ω is close to the above energy difference. In this case, function $L^{ab}_{\sigma}(\omega)$ has a pole singularity. The number of such poles determines the number of possible transitions manifested in the I–V characteristic. Significantly, in zero magnetic field, we have $L^{ab}_{\uparrow}(\omega) = L^{ab}_{\downarrow}(\omega)$ because the positions of the poles and the values of the representation parameters for both functions coincide in this case. The applica-

tion of a magnetic field leads to splitting of the energy levels. As a result, the change in the energy of the system upon a transition of an electron from a contact to the system becomes a function of the electron spin projection. Therefore, the number of the observed transitions accompanied with an increase in the number of steps on the I–V curve increases in the magnetic field. Since these peculiarities are manifested above all in function $L_\sigma^{ab}(\omega)$, we can demonstrate this effect as follows. Let us consider the terms

$$l_{2,8} = \frac{N_2 + N_8}{\omega - A/2 - \xi_d + h}, \quad l_{3,9} = \frac{N_3 + N_9}{\omega - A/2 - \xi_d - h},$$

appearing in functions $L_\uparrow^{ab}(\omega)$ and $L_\downarrow^{ab}(\omega)$ and corresponding to transitions (2, 8) and (3, 9). It can be seen that in zero magnetic field, the above terms have the same pole $\omega = \omega_0 = A/2 + \xi_d$ corresponding to these transitions. In a magnetic field, however, two transitions initiated by two poles ($\omega = \omega_0 \mp h$) appear. It is this scenario that determines the occurrence of additional steps on the I–V curves upon application of magnetic field. In addition, the peculiarities considered here underlie the modification of the dependence of the occupation numbers on the electric field upon the application of h (see Fig. 5 below). It should be noted that the qualitative pattern of the effect of the magnetic field for other terms of functions $L_\uparrow^{ab}(\omega)$ and $L_\downarrow^{ab}(\omega)$ does not differ from this pattern.

Constructing the system of equations for functions $D_{\alpha\beta}^{-+}(\omega)$ and $D_{\alpha\beta}^{++}(\omega)$ analogously and solving it, we obtain

$$W_\sigma^{-+}(\omega) = -\frac{M_\sigma^{-+}(\omega)}{\Delta_\sigma(\omega)}. \tag{40}$$

6. CURRENT AND SYSTEM OF QUANTUM KINETIC EQUATIONS FOR OCCUPATION NUMBERS

Using the expressions derived above for the spectral functions of the system, we arrive at the following formula for current:

$$I = e\sum_\sigma \int_{-\infty}^{\infty} \frac{d\omega}{2\pi\Delta_\sigma(\omega)} \times \left[Q_\sigma^{+-}\left(\omega + \frac{eV}{2}\right) P_\sigma^{-+}\left(\omega - \frac{eV}{2}\right) - Q_\sigma^{-+}\left(\omega + \frac{eV}{2}\right) P_\sigma^{+-}\left(\omega - \frac{eV}{2}\right) \right]. \tag{41}$$

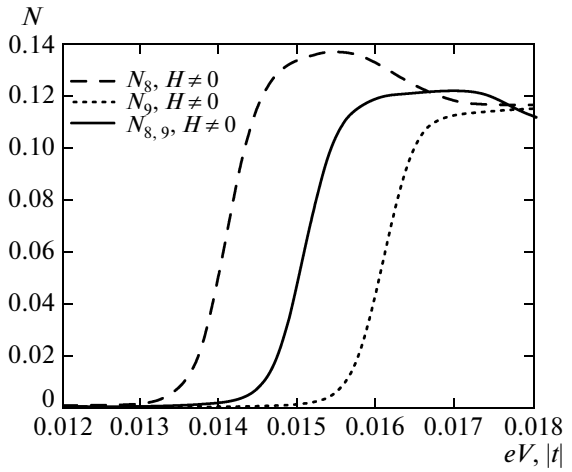

Fig. 5. Modification of the dependences of the occupation numbers $N_{8,9}(eV)$ in magnetic field $h = 5 \times 10^{-4}|t|$ for parameters from Fig. 4.

Writing the components of mass operator $M_\sigma^{ab}(\omega)$ in explicit form, we obtain

$$I_L = 2e\sum_\sigma \int_{-\infty}^{\infty} \frac{d\omega}{\pi}[n(\omega - eV) - n(\omega)] \times \frac{\Gamma_{L\sigma}(\omega)\Gamma_{R\sigma}(\omega)}{[L_\sigma^{-1}(\omega) - \Lambda_\sigma(\omega)]^2 + \Gamma_\sigma^2(\omega)}, \tag{42}$$

where

$$L_\sigma(\omega) = \sum_\alpha \frac{b_\alpha \gamma_\sigma^2(\alpha)}{\omega + E_\alpha - eV/2},$$
$$\Lambda_\sigma = \sum_k \frac{t_{Lk}^2}{\omega - \xi_{Lk\sigma}} + \sum_p \frac{t_{Rp}^2}{\omega - \xi_{Rp\sigma} - eV}. \tag{43}$$

Function Λ_σ is responsible for the radiation shift of the energy levels of the system due to the effect of the left and right contacts. As noted above, in discussing the terms in the Hamiltonian of the system, we use here the assumption that the contacts are broadband metals. This allows us in specific calculations to disregard the shift Λ_σ as well as the frequency dependence of level-broadening functions $\Gamma_\sigma = \Gamma_{L\sigma} + \Gamma_{R\sigma} = \pi(t_L^2 g_{L\sigma} + t_R^2 g_{R\sigma})$ [27]. In this expression, $t_{L(R)}$ is the parameter of electron hopping from the last site of the left (right) contact to the level of the magnetic atom and $g_{L(R)\sigma}$ is the spin-dependent density of states of the left (right) contact. An important property of expression (42) derived for the current is associated with its proportionality to product $t_L^2 t_R^2$ and, hence, meets the necessary physical requirements [13].

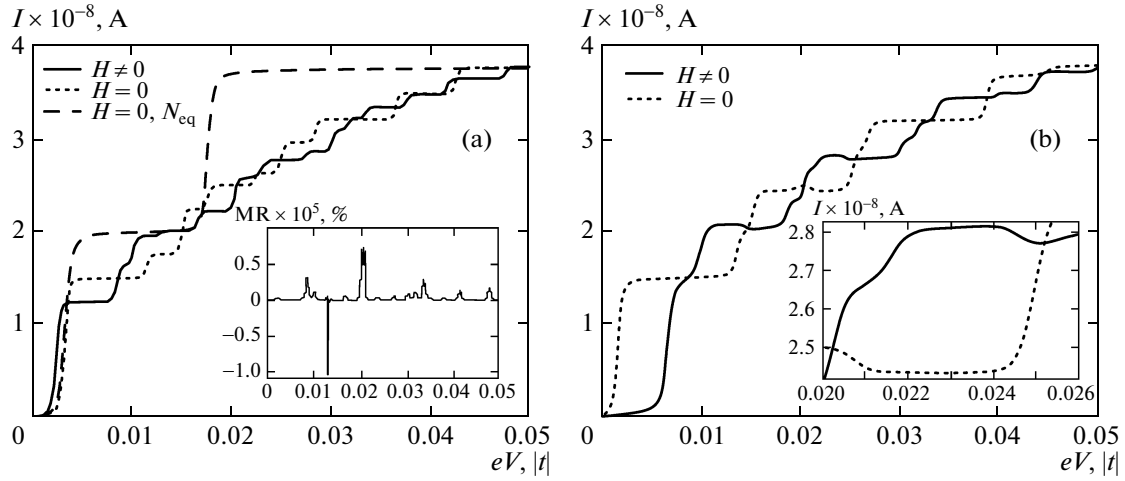

Fig. 6. I–V curves for a magnetic atom for parameters from Fig. 5: (a) $D = 0.003|t|$ and (b) $D = -0.003|t|$. The insets in (a) and (b) show the magnetoresistance of the structure and a segment on the I–V curve with a NCD.

To derive the system of kinetic equations for occupation numbers, we will use the relation

$$N_m = \frac{1}{2\pi i}\int_{-\infty}^{\infty} d\omega D_{\alpha\alpha}^{+-}(\omega). \tag{44}$$

Calculating function $D_{\alpha\alpha}^{+-}(\omega)$ in accordance with the technique described above, we obtain

$$N_m = \int_{-\infty}^{\infty}\frac{d\omega}{\pi}\left(\frac{b_\alpha\gamma_\sigma(\alpha)}{\omega_\alpha L_\sigma(\omega)}\right)^2 \times \frac{\Gamma_{L\sigma}(\omega)n(\omega) + \Gamma_{R\sigma}(\omega)n(\omega - eV)}{[L_\sigma^{-1}(\omega) - \Lambda_\sigma(\omega)]^2 + \Gamma_\sigma^2(\omega)}, \tag{45}$$

where $\omega_\alpha = \omega + E_\alpha - eV/2$. In writing this equation, we used the following property: in the collinear geometry of the problem considered here, only one of two parameters $\gamma_\uparrow(\alpha)$ and $\gamma_\downarrow(\alpha)$ of the representation for each one-fermion transition differs from zero. For this reason, we choose the value of spin projection σ for the quantities appearing in expression (45), such that $\gamma_\sigma(\alpha) \neq 0$.

We will confine further analysis to only the transport properties of the magnetic system for the regime of the tunnel coupling between the system and a contact at low temperatures. This case is observed in experiments most often [28, 29]. In the mathematical language, this regime corresponds to the fulfillment of the inequalities $T, \Gamma_\sigma \ll E_\alpha$, which indicates small values of the temperature and energy level broadening as compared to the spacing between these levels. In this case, we can write

$$N_m \approx \frac{b_\alpha}{\pi}\left[\arctan\left(\frac{W/2 + eV/2 - \omega_{0\alpha}}{\kappa_\alpha}\right) + \frac{\Gamma_{L\sigma}}{\Gamma_\sigma}\arctan\left(\frac{\omega_{0\alpha} - eV/2}{\kappa_\alpha}\right) + \frac{\Gamma_{R\sigma}}{\Gamma_\sigma}\arctan\left(\frac{\omega_{0\alpha} + eV/2}{\kappa_\alpha}\right)\right], \tag{46}$$

where the following notation has been introduced:

$$\omega_{0\alpha} = E_\alpha + \lambda_\alpha\kappa_\alpha, \quad \kappa_\alpha = \frac{b_\alpha\gamma_\sigma^2(\alpha)\Gamma_\sigma}{1 + \lambda_\alpha^2},$$

$$\lambda_\alpha = \sum_{\beta\neq\alpha}\frac{b_\beta\gamma_\sigma^2(\beta)\Gamma_\sigma}{E_\beta - E_\alpha}.$$

It can easily be verified that under the above assumptions, the main contribution to the tunnel current comes from diagonal terms ($I \approx \sum_\alpha I_{\alpha\alpha}$); therefore,

$$I \approx \frac{2e}{\pi}\sum_\alpha\frac{\Gamma_{L\sigma}\Gamma_{R\sigma}}{\Gamma_\sigma}b_\alpha\gamma_\sigma^2(\alpha) \times\left[\arctan\left(\frac{\omega_{0\alpha} + eV/2}{\kappa_\alpha}\right) - \arctan\left(\frac{\omega_{0\alpha} - eV/2}{\kappa_\alpha}\right)\right]. \tag{47}$$

7. TRANSPORT PROPERTIES OF A MAGNETIC IMPURITY

In numerical calculations, all energy parameters were measured in the units of $|t|$. It follows from experimental [30–32] and theoretical [33, 34] publications that the model parameters satisfy the following

relations: $|t_L|$, $|t_R| > |A|$, $|D|$, $|\varepsilon_d|$, $|h|$. This range of parameters also includes the relations for which the condition $\Gamma_\sigma \ll E_\alpha$ of the tunnel coupling between the system and the contacts is observed. Since $W \gg h$, we assume that $g_{L\sigma} = g_{R\sigma} = 1/W$ [27].

Let us first consider the results of numerically solving the set of kinetic equations for occupation numbers, which were determined under the condition $\sum_{i=1}^{12} N_i = 1$. Figure 4 shows the dependences of the nonequilibrium occupation numbers N of the states of the "electrons + magnetic impurity" system on the energy eV of the electric field for $h = 0$.

We assume for definiteness that in equilibrium ($t_L = t_R = 0$), the ground state of the system under investigation for $D > 0$ is the state free of electrons with $S^z = 0$, ψ_1 ($N_1 \approx 1$). Then, under nonequilibrium conditions in which multiple inelastic scattering processes are activated, the upper energy states of the magnetic impurity must be populated. This is demonstrated in Fig. 4. It can be seen that N_1 starts deviating considerably from the equilibrium value even at zero voltage. To find the reason for the peculiarities appearing in the behavior of the occupation numbers and the current for $V \neq 0$, we must analyze the corresponding analytic expressions (46) and (47). Since $W/2 \gg E_\alpha$, $eV/2 \gg \lambda_\alpha, \kappa_\alpha$, the main effects are observed in the range of $eV/2 \sim E_\alpha$. Indeed, disregarding small corrections to energy $E_\alpha < 0$ (> 0) of transition α, we can see that in the tunnel regime for $eV/2 < E_\alpha$ and $t_L = t_R$, the upper level remains unfilled, $N_m = 0$ ($N_n = 0$), and the contribution to the current from this transition is zero ($I_{\alpha\alpha} = 0$). In turn, when $eV/2 > E_\alpha$, the population of levels is the same ($N_n = N_m$) and the contribution to the current from such a channel is other than zero ($I_{\alpha\alpha} = 2e\Gamma_{L\sigma}\Gamma_{R\sigma}b_\alpha\gamma_\sigma^2(\alpha)/\Gamma_\sigma$). Let us return to Fig. 4. The lowest transition energy is $E_{3,5} \approx 0.0013$. However, with increasing V, in region $eV/2 \sim E_{3,5}$, no significant changes are observed in the population probability distribution of the levels and in the I–V characteristic (see the dotted curve in Fig. 6a below). This is due to the fact that lower-lying states $\psi_{4,5}$ (see the dashed curve in Fig. 4) are almost empty. The population of these states becomes significant only when the electric field energy approaches the doubled energy of the next transition ($E_{1,4} \approx -0.0017$). As a result, states $\psi_{4,5}$ and $\psi_{2,3}$ are populated simultaneously (dotted curve in Fig. 4). It can be seen that the corresponding step singularity appears on the I–V curve also.

The inset to Fig. 4 shows the arrangement of all energy levels of the system for the chosen parameters. Arrows with digits show possible transitions with a change in the number of electrons by unity. The transition number corresponds to the number of a step singularity on the curve. In particular, arrows with digits 1 and 2 denote the transitions between the states of the zero-

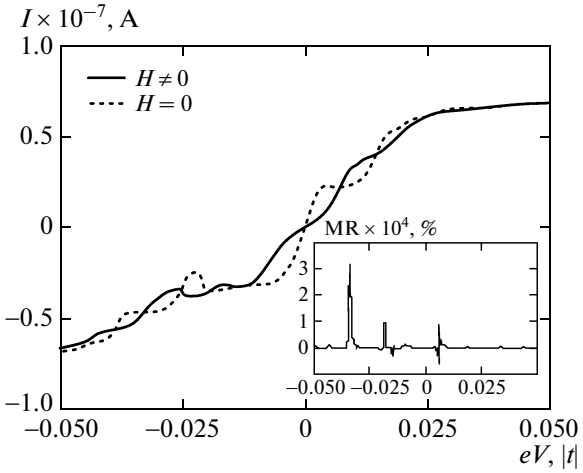

Fig. 7. Effect of asymmetry in the coupling of the magnetic atom with contacts on the I–V characteristic for the parameters from Fig. 5 and $t_L = t/25$, $t_R = t_L/4$, and $D = -0.003|t|$. The inset shows the magnetoresistance of the structure.

electron and one-electron sectors of the Hilbert space considered above. As the voltage increases, new and new channels corresponding to one-electron and two-electron states are involved in the transport. For large values of eV, the populations of all states become equiprobable. The I–V curve has the step form typical of the regime of weak coupling of the nanostructure with the contacts, which was observed in experiments [28, 29]. It is important that the disregard of nonequilibrium excitation of the magnetic atom as a result of inelastic scattering of charge carriers leads to a much simple I–V characteristic (see the dashed curve in Fig. 6a below).

When the magnetic field is applied, the degeneracy in energy for the states of the system with opposite projections of the total spin is removed in accordance with expression (12). Consequently, the energies of the transitions associated with these states also become different. In this case, the excited state with the total spin projection of the same polarity as that of the magnetic field is activated sooner than the state with the total spin projection of the opposite sign. This is depicted in Fig. 5, which shows the $N_{8,9}(eV)$ dependences disregarding (solid curve) and taking into account (dashed and dotted curves, respectively) the magnetic field. The nonequilibrium occupation numbers of other states that are degenerate for $h = 0$ behave analogously after the application of the magnetic field. As a result, the number of the Coulomb steps on the I–V curve increases, which is clearly seen from comparison of the solid ($h \neq 0$) and dotted ($h = 0$) curves in Fig. 6a. As a result of modification of the I–V characteristic, instead of the plateau on the I–V curve in zero magnetic field, current jumps can take place for $h \neq 0$. Thus, the system under investigation possesses a magnetoresistance MR = $(G(h)/G(0) - 1) \times 100\%$ ($G =$

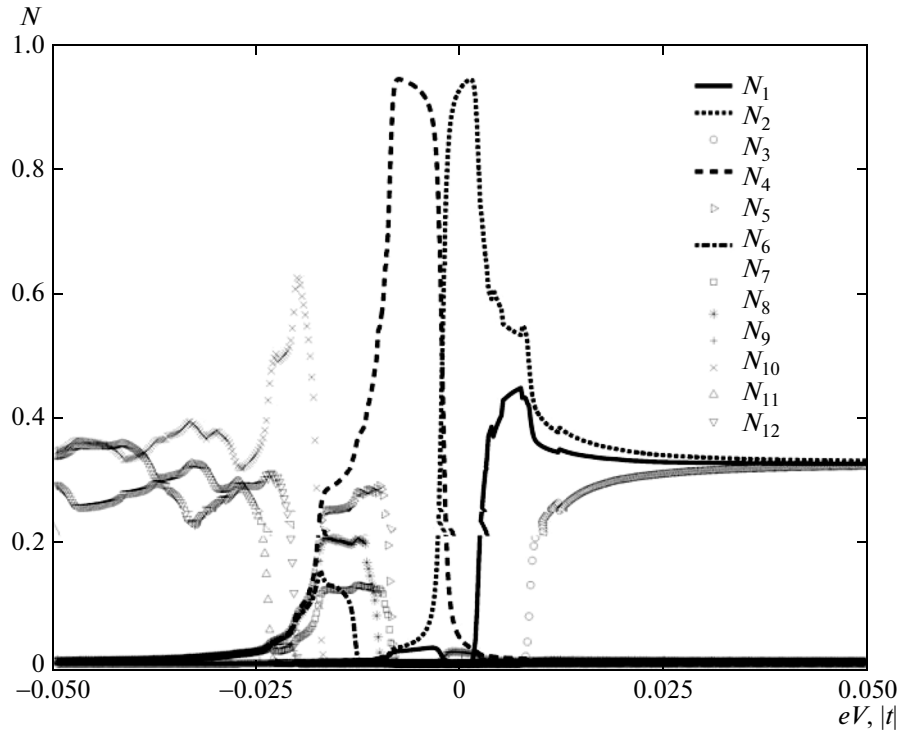

Fig. 8. Nonequilibrium occupation numbers of the system in the case of an asymmetric coupling of the magnetic atom with the contacts for the parameters from Fig. 5 and $t_L = t/50$ and $t_R = t_L/10$.

dI/dV is the differential conductivity) with an amplitude that can reach 10^5% (see the inset to Fig. 6a).

The I–V curves in Fig. 6b for $h = 0$ and $h \neq 0$ (the dotted and solid curves, respectively) plotted for the opposite sign of the anisotropy parameter of the magnetic impurity ($D < 0$) contain segments with a negative differential conductivity (NDC). Two such segments are shown in detail in the inset to Fig. 6b. As noted above, for electric field energy $eV/2 \sim E_\alpha$, the I–V curve exhibits a jump on the order of $I_{\alpha\alpha} = 2e\Gamma_{L\sigma}\Gamma_{R\sigma}b_\alpha\gamma_\sigma^2(\alpha)/\Gamma_\sigma$, which is associated with the population of a new excited state of the system. However, since the completeness condition must be satisfied in the nonequilibrium regime, occupation numbers differing from zero at lower voltages decrease. For this reason, the total current may decrease even when an additional channel for the electron transport is activated. As a result, the condition for the emergence of a NDC has the form

$$\sum_\beta I_{\beta\beta}(V_1) > \sum_\beta [I_{\beta\beta}(V_2) + I_{\alpha\alpha}(V_2)], \quad V_1 < V_2. \quad (48)$$

Thus, by changing the crystal surroundings of a magnetic atom or a molecule (e.g., by placing them in topologically nonequivalent positions on the substrate [17]), we can substantially modify the transport properties of atomic-scale systems.

If the mutual variation of the "new" and "old" occupation numbers is especially significant, this leads to enhancement of the NDC effect. Such a situation is observed in the case of asymmetry in the tunnel coupling of contacts with the structure ($t_L > t_R$, $\Gamma_{L\sigma} \gg \Gamma_{R\sigma}$). Figure 7 shows the I–V curves for an asymmetric coupling between the magnetic structure and the contacts in zero (dotted curve) and nonzero (solid curve) magnetic fields. In the range $-eV/2 \sim E_{6,11} \approx 0.01$, the current changes more strongly than in an analogous situation ($eV/2 \sim E_{6,11}$) for $t_L = t_R$ (see the inset to Fig. 6b).

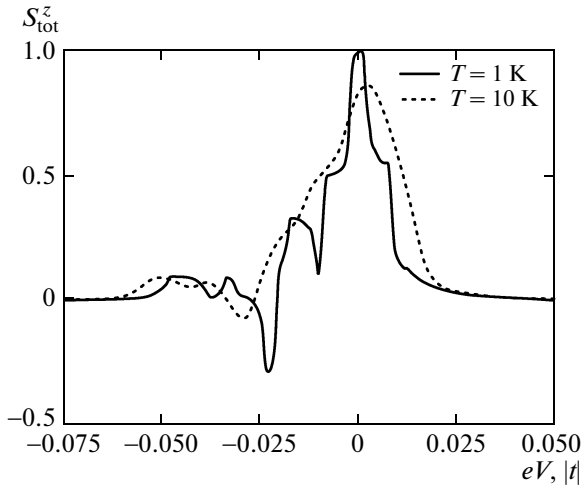

Fig. 9. Projection of total spin S^z_{tot} of the system as a function of the electric field energy eV for the parameters from Fig. 8.

To find the reason for this difference, let us analyze the evolution of the population of states of the system. For $V < 0$, the electron flow to the region of the right contact dominates. However, under the conditions considered here, the transition of electrons from the level of the system to the right contact is suppressed to a considerable extent, and for large absolute values of V, electrons are accumulated in the system; as a result, predominant population of two-electron states (N_{10}, N_{11}, and N_{12}) takes place with a simultaneous sharp decrease in the population of the remaining states (see region $eV < -0.02$ in Fig. 8). Therefore, the modulus of the current decreases by a larger value as compared to the case of a symmetric tunnel coupling ($t_L = t_R$). It is important that such an NDC effect is not observed upon the application of the field of the opposite polarity ($eV/2 \sim E_{6,11}$). For $V > 0$, only zero-electron states (N_1, N_2, and N_3) are mainly populated for the above reasons. As a result, the total current remains almost unchanged for $eV \sim E_{6,11}$ because this transition occurs between one- and two-electron states.

Concluding the section, we note that in the system under investigation, switching between the states with different projections of total spin S^z_{tot} is achieved with a high probability. Figure 9 shows the $S^z_{\text{tot}}(eV)$ dependences at temperatures $T = 1$ K (solid curve) and $T = 10$ K (dashed curve). The behavior of S^z_{tot} at lower temperatures indicates that for electric field energies $-0.075 \le eV \le -0.05$, the system is in the superposition of three two-electron states with zero total spin projections. In the interval $-0.01 < eV < -0.005$, the total spin projection is 1/2; for $-0.005 < eV < 0.005$, the zero-electron states with $S^z_{\text{tot}} = 1$ is realized with a probability of 90%. For $eV = 0.05$, three states with $S^z_{\text{tot}} = 0$ are predominantly populated again. As expected, enhancement of thermal fluctuations in the system suppresses the effect of switching between spin states (see dashed curve in Fig. 9). Such a possibility of controlling the magnetic state of the object at atomic level under the action of an external electric field may turn out to be promising for applications of data recording and storage in nanoelectronics.

8. CONCLUSIONS

The development of the theory of quantum transport of electrons through atomic-scale magnetic structures performed in this study taking into account multiple scattering is based on application of the Keldysh method and the diagram technique for the Hubbard operators. Using the atomic representation, we have demonstrated that calculation of the tunnel current can be reduced to determining the spectral functions of the object. These functions were calculated using the nonequilibrium diagram technique for the Hubbard operators, applied to a multilevel system with a nonequidistant energy spectrum and with an effective time-dependent interaction.

This concept was used in analyzing the transport properties of a magnetic impurity in the tunnel junction with two paramagnetic metals in an external magnetic field at finite temperatures. The effect of the substrate was treated as the action of the crystal field on the states of the magnetic impurity and was simulated by introducing the term describing one-ion anisotropy with parameter D into the Hamiltonian.

The main task in our investigations is associated with taking into account multiple scattering of conduction electrons from the magnetic impurity in the case of a nonequilibrium distribution of the population of states (occupation numbers). As a result of such processes, the main contribution to the quantum transport of electrons comes from the states that were not populated in the case of the equilibrium distribution, and the corresponding current channel would be ineffective. Thus, multiple scattering processes make possible transitions of the system from excited states to even higher-lying energy states [10] and are manifested as a renormalization of the I–V characteristics.

Numerical solution of the system of kinetic equations for occupation numbers followed by calculation of the current showed that the I–V curve of the magnetic atomic system has singularities in the form of steps typical of the Coulomb blockade effect and observed in earlier experiments [28, 29]. It is shown that application of a magnetic field, when the degeneracy in the energy of transitions between the states for electrons with spin projections of $+1/2$ and $-1/2$ is removed, the I–V characteristics acquire experimentally observed fine singularities in the form of new inflections. As a result, a high magnetoresistance (MR $\sim 10^5$ %) appears at the impurity atom.

Our calculations show that for electric field energies on the order of transition energy E_α, the NDC effect occurs in the system under investigation. In the NDC formation, the following two factors are significant. The first is associated with the above-mentioned effect of multiple inelastic scattering. The second factor is due to concordant types of behavior of nonequilibrium occupation numbers of the system, when the requirement that the sum of these numbers must be equal to unity is imposed in view of completeness of the diagonal Hubbard operators. We have demonstrated that the NDC effect in practical realization can be enhanced by changing the crystal surroundings of the magnetic impurity or due to asymmetric coupling with the contacts. In the latter case, we have demonstrated the possibility of switching between the configurations of the "magnetic impurity + electrons" system, in which electrons have different projections of the total spin.

Analysis of the effect of multiple scattering on the quantum transport of electrons through an anisotropic atom has been performed for a particular case when the magnetic field direction is collinear to the anisotropy axis. As noted above, the solution of the system of

equations for nonequilibrium Green's function is substantially simplified in this case.

In the noncollinear situation, the total spectral functions of the system cannot be generally classified using the projection of the spin moment. In this case, each function of the system contains all transitions corresponding to the representation parameters $\gamma_\uparrow(\alpha)$ and $\gamma_\downarrow(\alpha)$. Under such conditions, an increase in the magnetic field affects the shift of transition energies as well as the intensities of the transitions. It should be emphasized, however, that the qualitative features of the effect of the magnetic field on the transport characteristics of the system under investigation with allowance for multiple scattering effects are fully manifested in the collinear geometry.

ACKNOWLEDGMENTS

This work was performed under the Program "Quantum Mesoscopic and Disordered Systems" of the Presidium of the Russian Academy of Sciences and supported financially by the Russian Foundation for Basic Research (project nos. 13-02-00523, 13-02-98013, and 14-02-31280). The work of one of coauthors (S.V.A.) was supported by grant no. MK-526-526.2013.2 of the President of the Russian Federation and scholarship SP-6361.2013.5 of the President of the Russian Federation.

REFERENCES

1. S. N. Vdovichev, B. A. Gribkov, S. A. Gusev, A. Yu. Klimov, V. L. Mironov, I. M. Nefedov, V. V. Rogov, A. A. Fraerman, and I. A. Shereshevskii, JETP Lett. **94** (5), 386 (2011).
2. I. V. Rozhansky, N. S. Averkiev, and E. Lahderanta, Phys. Rev. B: Condens. Matter **85**, 075315 (2012).
3. Y. Makhlin, G. Schon, and A. Shnirman, Rev. Mod. Phys. **73**, 357 (2001).
4. V. F. Gantmakher and V. T. Dolgopolov, Phys.—Usp. **53** (1), 1 (2010).
5. A. K. Feofanov, V. A. Oboznov, V. V. Bol'ginov, J. Lisenfeld, S. Poletto, V. V. Ryazanov, A. N. Rossolenko, M. Khabipov, D. Balashov, A. B. Zorin, P. N. Dmitriev, V. P. Koshelets, and A. V. Ustinov, Nat. Phys. **6**, 593 (2010).
6. J. Park, A. N. Pasupathy, J. I. Goldsmith, C. Chang, Y. Yaish, J. R. Petta, M. Rinkoski, J. P. Sethna, H. D. Abruña, P. L. McEuen, and D. C. Ralph, Nature (London) **417**, 722 (2002).
7. A. J. Heinrich, J. A. Gupta, and C. P. Lutz, Science (Washington) **306**, 466 (2004).
8. L. Besombes, Y. Leger, L. Maingault, D. Ferrand, H. Mariette, and J. Cibert, Phys. Rev. Lett. **93**, 207403 (2004); L. Besombes, Y. Leger, L. Maingault, D. Ferrand, H. Mariette, and J. Cibert, Phys. Rev. B **71**, 161307 (2005).
9. C. F. Hirjibehedin, C. P. Lutz, and A. J. Heinrich, Science (Washington) **312**, 1021 (2006).
10. S. Loth, K. von Bergmann, M. Ternes, A. F. Otte, C. P. Lutz, and A. J. Heinrich, Nat. Phys. **6**, 340 (2010).
11. S. Loth, S. Baumann, C. P. Lutz, D. M. Eigler, and A. J. Heinrich, Science (Washington) **335**, 196 (2012).
12. K. Kikoin, and Y. Avishai, Phys. Rev. Lett. **86**, 2090 (2001).
13. P. I. Arseyev, N. S. Maslova, and V. N. Mantsevich, JETP Lett. **94** (5), 390 (2011).
14. H. Ueba, T. Mii, and S. G. Tikhodeev, Surf. Sci. **601**, 5220 (2007).
15. P. I. Arseev and N. S. Maslova, Phys.—Usp. **53** (11), 1151 (2010).
16. N. Tsukahara, K.-I. Noto, M. Ohara, S. Shiraki, N. Takagi, Y. Takata, J. Miyawaki, M. Taguchi, A. Chainani, S. Shin, and M. Kawai, Phys. Rev. Lett. **102**, 167203 (2009).
17. A. F. Otte, M. Ternes, K. von Bergmann, S. Loth, H. Brune, C. P. Lutz, C. F. Hirjibehedin, and A. J. Heinrich, Nat. Phys. **4**, 847 (2008).
18. V. V. Val'kov, S. V. Aksenov, and E. A. Ulanov, JETP Lett. **98** (7), 403 (2013).
19. R. O. Zaitsev, Sov. Phys. JETP **41** (1), 100 (1975).
20. R. O. Zaitsev, Sov. Phys. JETP **43** (3), 574 (1976).
21. L. V. Keldysh, Sov. Phys. JETP **20**, 1018 (1964).
22. R. O. Zaitsev, *Introduction to the Modern Kinetic Theory: A Series of Lectures* (KomKniga, Moscow, 2007; URSS, Moscow, 2014).
23. J. Fransson, O. Eriksson, and I. Sandalov, Phys. Rev. Lett. **88**, 226601 (2002).
24. V. V. Val'kov and S. V. Aksenov, J. Exp. Theor. Phys. **113** (2), 266 (2011); V. V. Val'kov, S. V. Aksenov, and E. A. Ulanov, J. Exp. Theor. Phys. **116** (5), 854 (2013).
25. V. V. Val'kov and D. M. Dzebisashvili, J. Exp. Theor. Phys. **107** (4), 679 (2008).
26. V. V. Val'kov and T. A. Val'kova, Sov. J. Low Temp. Phys. **11** (9), 524 (1985).
27. S. G. Tikhodeev and H. Ueba, in *Problems of Condensed Matter Physics*, Ed. by A. L. Ivanov and S. G. Tikhodeev (Clarendon, Oxford, 2008).
28. H. B. Heersche, Z. de Groot, J. A. Folk, H. S. J. van der Zant, C. Romeike, M. R. Wegewijs, L. Zobbi, D. Barreca, E. Tondello, and A. Cornia, Phys. Rev. Lett. **96**, 206801 (2006).
29. M.-H. Jo, J. E. Grose, K. Baheti, M. Deshmukh, J. J. Sokol, E. M. Rumberger, D. N. Hendrickson, J. R. Long, H. Park, and D. C. Ralph, Nano Lett. **6**, 2014 (2006).
30. J. Göres, D. Goldhaber-Gordon, S. Heemeyer, M. A. Kastner, H. Shtrikman, D. Mahalu, and U. Meirav, Phys. Rev. B: Condens. Matter **62**, 2188 (2000).
31. I. G. Zacharia, D. Goldhaber-Gordon, G. Granger, M. A. Kastner, Yu. B. Khavin, H. Shtrikman, D. Mahalu, and U. Meirav, Phys. Rev. B: Condens. Matter **64**, 155311 (2001).
32. C. F. Hirjibehedin, C.-Y. Lin, A. F. Otte, M. Ternes, C. P. Lutz, B. A. Jones, and A. J. Heinrich, Science (Washington) **317**, 1199 (2007).
33. K. Park, and M. R. Pederson, Phys. Rev. B: Condens. Matter **70**, 054414 (2004).
34. F. Qu and P. Hawrylak, Phys. Rev. Lett. **95**, 217206 (2005).

Translated by N. Wadhwa